NASA CR134923

EFFECT OF DESIGN FACTORS ON SURFACE TEMPERATURE AND WEAR IN DISK BRAKES

J. J. Santini

F. E. Kennedy

F. F. Ling

TRIBOLOGY LABORATORY
DEPARTMENT OF MECHANICAL ENGINEERING,
AERONAUTICAL ENGINEERING & MECHANICS
RENSSELAER POLYTECHNIC INSTITUTE
TROY, NEW YORK 12181

MAY 1976

Prepared for
AEROSPACE SAFETY RESEARCH AND DATA INSTITUTE
LEWIS RESEARCH CENTER
NATIONAL AERONAUTICS AND SPACE ADMINISTRATION
CLEVELAND, OHIO 44135

Under

NASA Grant NGR 33-018-152

H. Schmidt, Program Manager
R. C. Bill, Technical Advisor

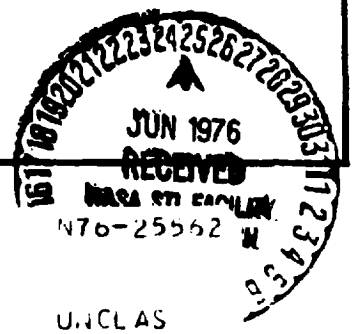

1. Report No.	2. Government Accession No.	3. Recipient's Catalog No.
NASA CR 134923		

4. Title and Subtitle	5. Report Date
Effect of Design Factors on Surface Temperature and Wear in Disk Brakes	May 1976
	6. Performing Organization Code

7. Author(s)	8. Performing Organization Report No.
J. J. Santini F. E. Kennedy F. F. Ling	

9. Performing Organization Name and Address	10. Work Unit No.
Rensselaer Polytechnic Institute Troy, New York 12181	11. Contract or Grant No. NGR 33-018-152

12. Sponsoring Agency Name and Address	13. Type of Report and Period Covered
National Aeronautics and Space Administration Washington, D.C. 20546	Contractor Report
	14. Sponsoring Agency Code

15. Supplementary Notes

Sponsored by Aerospace Safety Research and Data Institute, Lewis Research Center
H. Schmidt - Program Manager
R. C. Bill - Technical Advisor

16. Abstract

This report presents the results of an experimental investigation of the temperatures, friction, wear and contact conditions that occur in high-energy disk brakes. Surface and near-surface temperatures were monitored at various locations in a caliper disk brake during drag-type testing, with friction coefficient and wear rates also being determined. The recorded transient temperature distributions in the friction pads and infrared photographs of the rotor disk surface both showed that contact at the friction surface was not uniform, with contact areas constantly shifting due to nonuniform thermal expansion and wear.

The effect of external cooling and of design modifications on friction, wear and temperatures were also investigated. It was found that significant decreases in surface temperature and in wear rate can be achieved without a reduction in friction either by slotting the contacting face of the brake pad or by modifying the design of the pad support to improve pad compliance. Both design changes result in more uniform contact conditions on the friction surface.

17. Key Words (Suggested by Author(s))	18. Distribution Statement
Wear Aircraft Brake Design Surface Temperatures	Unclassified - unlimited

19. Security Classif. (of this report)	20. Security Classif. (of this page)	21. No. of Pages	22. Price*
Unclassified	Unclassified	38	

* For sale by the National Technical Information Service, Springfield, Virginia 22161

FOREWORD

This work was conducted as part of NASA Grant NGR 33-018-152 from the Office of University Affiars, Washington, D.C. 20546. Dr. R.C. Bill of NASA is the current project manager. Dr. F.F. Ling, Chairman of RPI's Department of Mechanical Engineering, Aeronautical Engineering & Mechanics, was the principal investigator.

Acknowledgement is made of the helpful suggestions given during the course of the investigation by Mr. C. David Miller of NASA, the former project monitor, and by Mr. M.B. Peterson of RPI's Tribology Laboratory.

TABLE OF CONTENTS

SECTION 1

SUMMARY

This report presents the results of an experimental investigation of the temperatures, friction, wear and contact conditions that occur in high-energy disk brakes. Surface and near-surface temperatures were monitored at various locations in a caliper disk brake during drag-type testing, with friction coefficient and wear rates also being determined. The recorded transient temperature distributions in the friction pads and infrared photographs of the rotor disk surface both showed that contact at the friction surface was not uniform, with contact areas constantly shifting due to nonuniform thermal expansion and wear.

The effect of external cooling and of design modifications on friction, wear and temperatures were also investigated. It was found that significant decreases in surface temperature and in wear rate can be achieved without a reduction in friction either by slotting the contacting face of the brake pad or by modifying the design of the pad support to improve pad compliance. Both design changes result in more uniform contact conditions on the friction surface.

SECTION 2

INTRODUCTION

Because of their ability to transform a large amount of kinetic energy to thermal energy in a short time, disk brakes are used on nearly all aircraft. The increased size and greater speeds of aircraft in recent years has required disk brakes to absorb more and more thermal energy, while at the same time maintaining good performance without much increase in size. Attempts to satisfy these requirements of greater heat capacity and braking performance have led to development of new friction materials that can absorb large amounts of heat while maintaining good frictional properties (Refs.1-3).

In addition to the development of better friction materials, however, the search for higher capacity, more efficient and safer disk brakes must also include the development of brake configurations that enable maximum advantage to be made of the new materials. This paper is concerned with this latter objective.

Although high temperatures are one of the biggest problems encountered in disk brakes, contributing as they do to rapid wear and poor braking performance, very little brake temperature data has been published. In addition, little is known about the actual contact conditions occurring on the friction surfaces during braking. This test program was set up in order to gather information about the actual temperature distribution on or near the sliding surfaces of disk brakes. The information was gathered during drag-type tests of a caliper disk brake on a specially built test rig. Commercially available, sintered, metal-based friction materials were utilized in the brake.

From the transient temperature data a great deal could be learned about the transient changes in contact that occur on the friction surface. Such contact area changes in high energy sliding situations have been known to exist for a number of years (Refs. 4,5) and have recently been associated with thermo-elastic instabilities on the sliding surfaces (Refs. 6,7).

After determination of the temperatures, friction coefficient, and wear rate of a conventional brake configuration, several modified friction pad

designs were tested in order to see if more uniform contact, lower surface temperatures and lower wear rates could be achieved.

SECTION 3

APPARATUS AND MATERIALS

The test apparatus shown in Figure 1 was built especially for this investigation in the Tribology Laboratory of Rensselaer Polytechnic Institute. Rotational power is provided to the brake rotor disk by a 40 horsepower (30 KW) AC electric motor with a rotational speed of 1750 rpm. The rotor disk was machined from 17-22AS steel and heat treated to a hardness of Rc 44-Rc50. The disk thickness was .36 inches (0.00915 m).

A commercial caliper brake was attached by means of a torque lever arm to the splined stationary shaft, which was aligned with the rotating motor shaft. The two caliper brake friction pads were of the type used in a large commercial aircraft brake. These trapezoidal-shaped pads consist of a sintered, copper-based friction material inside a steel cup. The pertinent geometrical and physical properties of the brake pads are given in Table 1.

The surface area of the pads was 6.2 in^2 (.004 m^2) and the thickness (before testing) was 0.24 in (.0061 m). The rear (noncontacting) surfaces of the friction pads were modified slightly to accept thermocouples. A regulated, oil-mist lubricated, compressed air supply was used to actuate the brakes. This pneumatic circuit was activated by a solenoid valve, with the duration of the brake application being controlled by a timer switch.

The monitoring equipment employed in the tests is shown schematically in Figure 2. Four strain gages were mounted parallel to the principal axes on the stationary shaft to continuously monitor frictional torque. A strain gage pressure transducer was used to measure the pressure applied to the brake pistons. The rotational velocity of the rotor disk was monitored by a DC tachometer generator.

Temperature measurements were made by six chromel-alumel thermocouples inserted at various locations in one of the two friction pads. The thermocouples were inserted through the back of the friction pad to within .01" - .03" (.00025 m - .000762 m) of the friction surface, thus enabling determination of temperatures very close to the sliding interface. A typical thermocouple installation is shown in Figure 3. The location of the thermocouples in relation

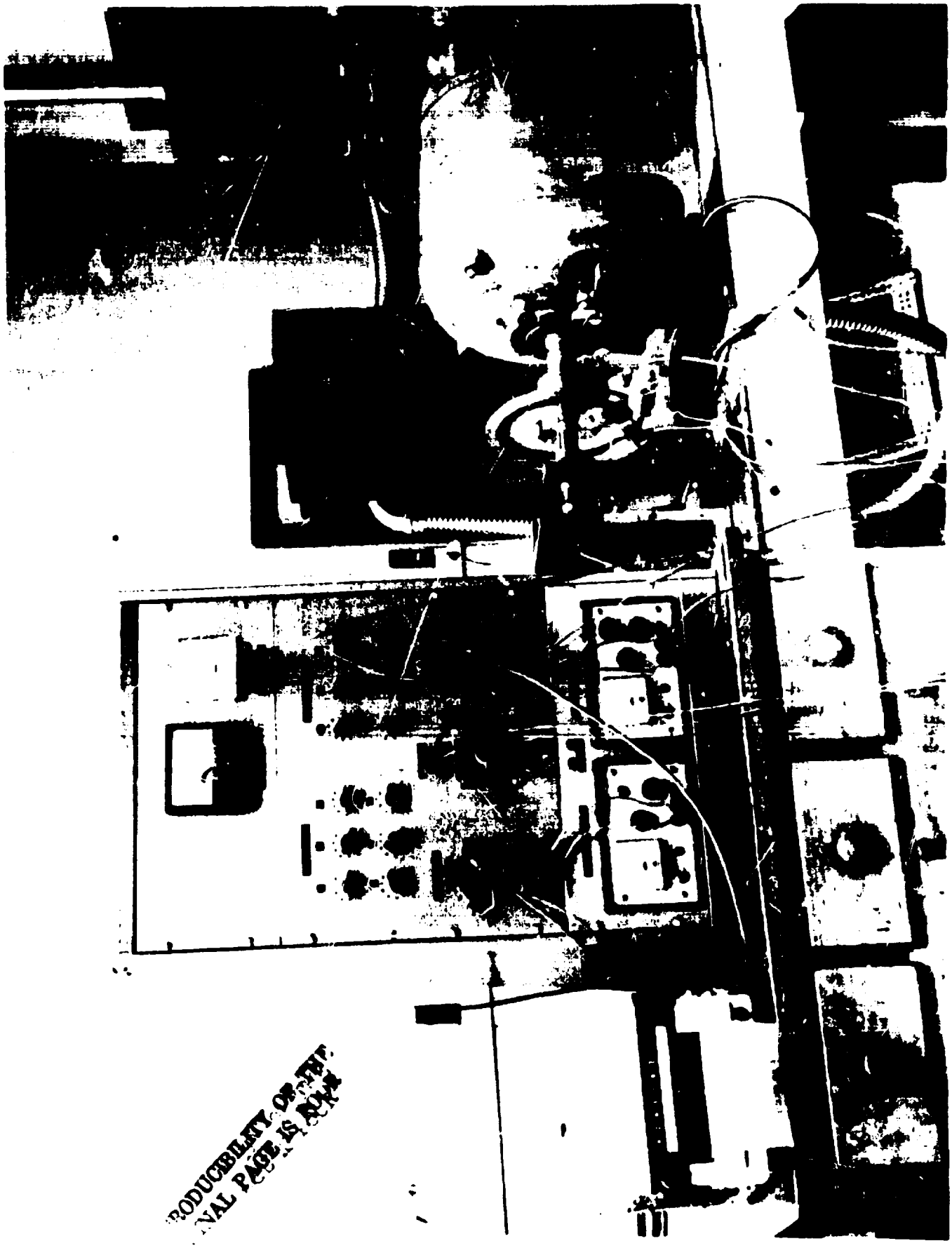

Figure 1. Disk brake test apparatus

TABLE 1

PERTINENT PROPERTIES OF STANDARD BRAKE PAD

	Engineering	C.G.S.	S.I.
Usable Contact Area	6.2 in^2	39.9	.00399
Geometric Shape	Trapezoidal	Trapezoidal	Trapezoidal
Average Weight	.346 lbs	157.	.157
Density	.177 lbs/in^3	4.9	$.0049 \times 10^6$
Specific Heat	$.125 \frac{BTU}{lb\ m\ ^\circ F}$	.125	$.523 \times 10^3$
Thermal Conductivity	$.254 \times 10^{-3} \frac{BTU}{in\ sec\ ^\circ F}$	.045	$.188 \times 10^2$
Thermal Diffusivity	$.0115 \frac{in^2}{sec}$	.0734	7.34×10^{-6}
Thickness (Total)	.24 in	.61	.0061
Tensile Strength	3000 psi	2.067×10^7	2.067×10^8
Compressive Strength	14,000 psi	9.646×10^7	9.646×10^8
Linear Thermal Expansion	$.37 \frac{in}{in}/^\circ F$	$.666 \times 10^{-4}$	$.666 \times 10^{-4}$

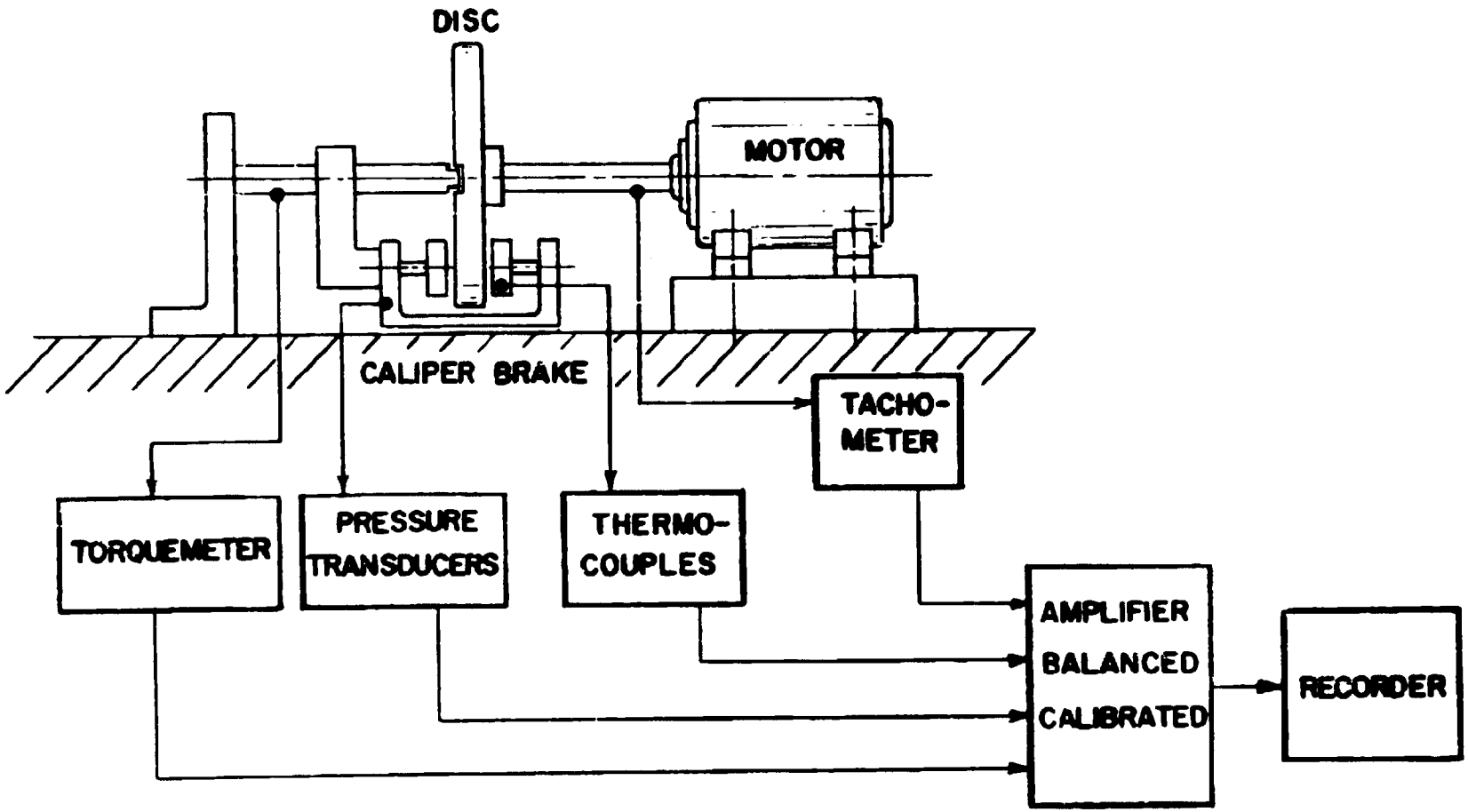

Figure 2 Schematic diagram of test monitoring equipment

to the pad geometry is shown in Figure 4. During any one test series, six thermocouples were utilized, with the six locations being chosen from the eight possibilities labelled 1-8 in Figure 4. Although continuous monitoring of rotor disk temperature was not done, occasional use was made of infrared photography during the tests and of temperature-indicating crayons after the test runs for determining disk surface temperature.

All monitoring devices were carefully calibrated before the test series and the calibrations were checked occasionally during the investigation. All electrical signals from the devices were continuously recorded on a 12-channel oscillograph during each test run.

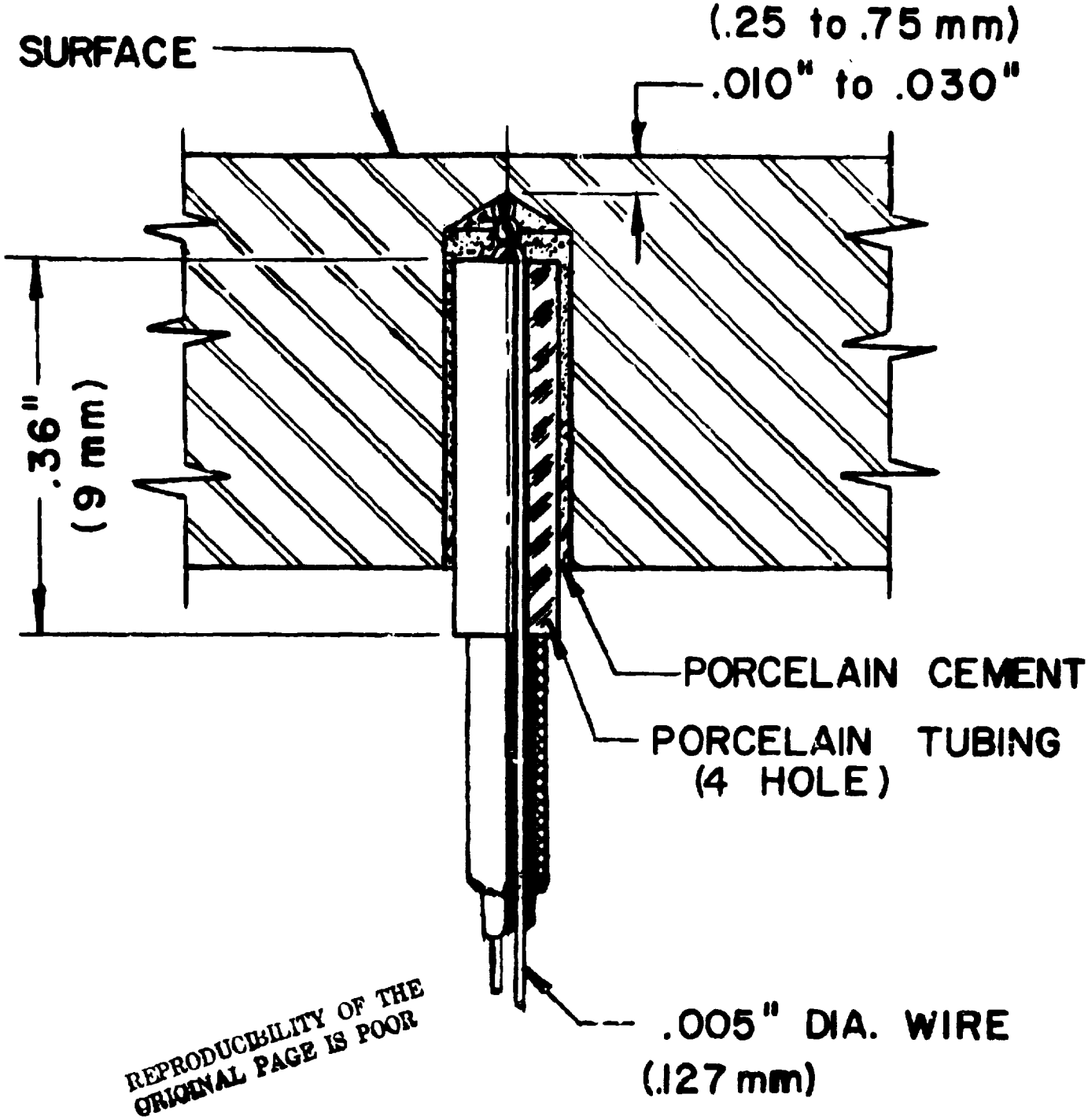

Figure 3 Typical thermocouple installation

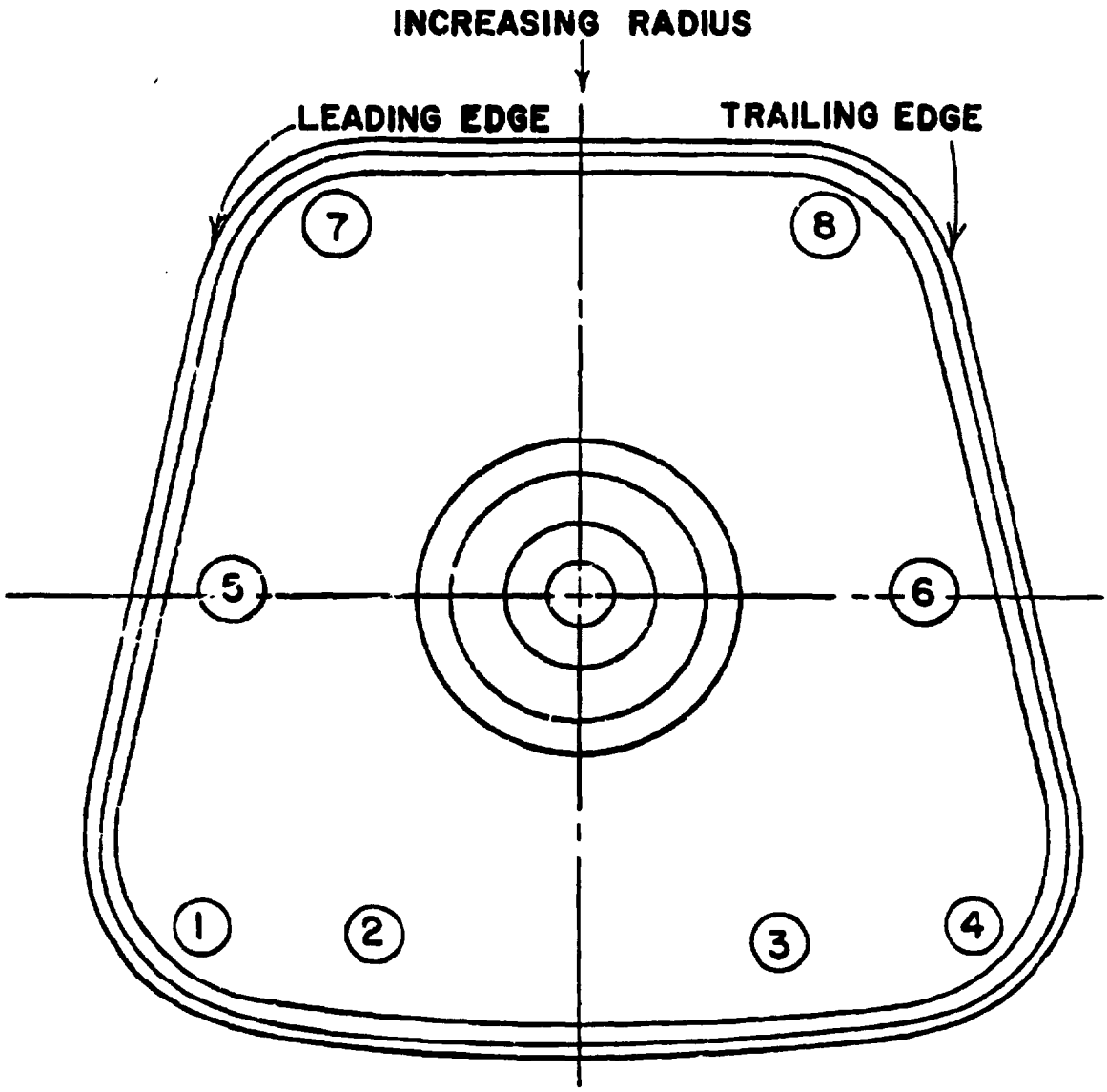

Figure 4. Thermocouple locations

SECTION 4

EXPERIMENTAL PROCEDURE

The experimental program consisted of three test series, each composed of 50 test runs. In the first test series, labelled series A, the friction pads were the standard configuration, as obtained from a brake manufacturer. After results of this first series had been analyzed, two design modifications were proposed, based on knowledge obtained from series A. These two modifications, which will be discussed later in this paper, were tested as series C and series R.

A new rotor disk and a pair of new friction pads were used for each test series. Before the rotor disk was mounted at the beginning of a series the sliding surfaces of the disk were ground finished and were cleaned using 2-propanol fluid. The new friction pads were cleaned and weighed before being put into place at the beginning of a test series. The pads were removed at regular intervals during the series to be weighed for wear rate determination. Except for manual removal of loose wear particles from the pads before weighing, no cleaning of either pad or disk was done during the test series in order to try to duplicate in situ conditions.

Each of the 50 test runs in a series was of 20 seconds duration. During the run a constant normal load of 400 lbs (1780 newtons) was applied to each friction pad by means of the piston behind the pad. This load was small enough that the power capacity of the electric motor was not exceeded and the rotational speed of the motor and rotor disk remained relatively constant at 1750 rpm. This resulted in a sliding velocity of 47.4 ft/sec (14 5 m/sec) at the inside radius of the friction pad and 89 ft/sec (27.1 m/sec) at the outside radius. The frictional work done by the pair of friction pads during each 20-second run was approximately 25% greater than the work done by a similar pair of pads in a normal landing of a large jet airliner.

Oscillograph traces were recorded continuously during each 20 second test for the tachometer, torquemeter, pressure transducer, and all six thermocouples. The test equipment was located in a temperature- and humidity-controlled laboratory, so all tests were run in the same environmental conditions.

The infrared photographs used to determine disk surface temperatures were taken with the laboratory completely darkened. The negatives were reduced using the densitometer technique and were calibrated by comparison with infrared photographs taken of similar 17-2 AS steel specimens heated to known temperatures. At the end of each test run the motor was shut off and all brake components were allowed to cool to room temperature before the next run.

SECTION 5

RESULTS AND DISCUSSION

5.1 Results for Standard Pad Configuration

The tests of series A were conducted to investigate the behavior of the standard brake pad configuration and to serve as a baseline for comparison with the modified configurations tested in series C and R. Six thermocouples were used to monitor pad temperature, with thermocouple positions 1,4,5,6,7 and 8 (Figure 4) being utilized.

The continuous oscillograph traces of temperature vs. time obtained for each thermocouple pointed out that a significant transient temperature gradient existed between different points on the contact surface. Although the temperature traces varied for different test runs, an averaging of the test results for each of the six positions revealed the existence of a definite pattern. The complete temperature - time traces for 25 test runs were averaged for each thermocouple position and the results are plotted in Figures 5a and 5b. It can be noted from the curves that during the first few seconds of brake application the temperatures at thermocouple positions 1 and 4 increase rapidly, while slower increases are noted at the other positions. This indicates that contact is initially most severe near the outside radius of the pad. Within a few seconds, the temperature at points 7 and 8 (near the inside radius) increases, while temperatures at positions 1 and 4 decrease. This indicates a transfer of contact from the outside to the inside of the pad. Later, points 1 and 4 show another temperature rise and then points 5 and 6 at the mid-radius increase more rapidly.

Although the greatest temperature differences in Figures 5a and 5b are between points on different radii, a temperature gradient across the pad in the tangential direction can also be noted. In general, points near the trailing edge (Figure 5b) have higher temperatures than those near the leading edge (Figure 5a) but again some transient fluctuations are observed.

The phenomenon of shifting contact area was also noted in infrared photographs taken of the rotating disk during a test. Figure 6 shows infrared photos taken at one second intervals near the end of a test run. Significant

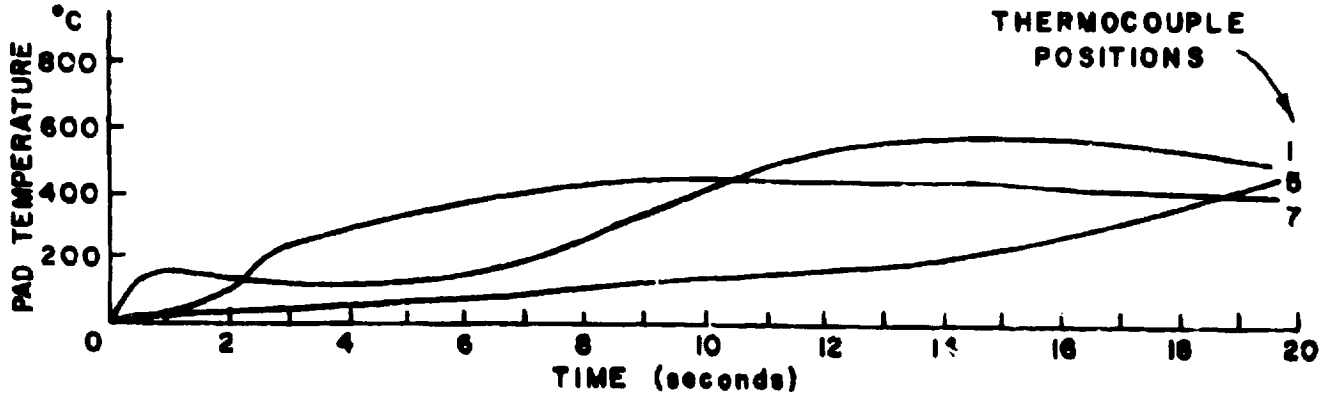

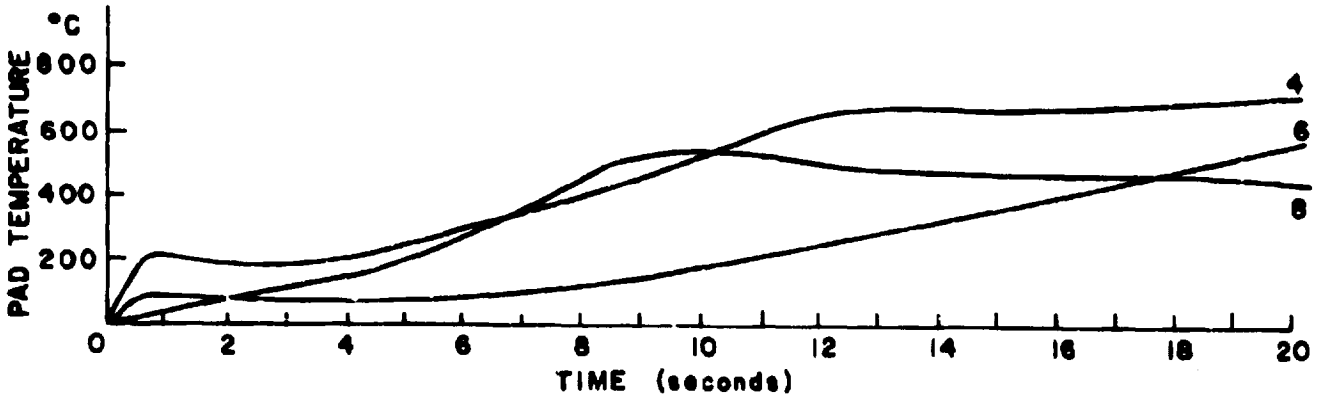

Figures 5a and b. Pad near-surface temperature vs. time averaged for 25 test runs. Series A - standard brake pad.
5a. (above) Temperatures for thermocouple positions 1,5,7 (leading edge)
5b. (below) Temperatures for thermocouple positions 4,6,8 (trailing edge)

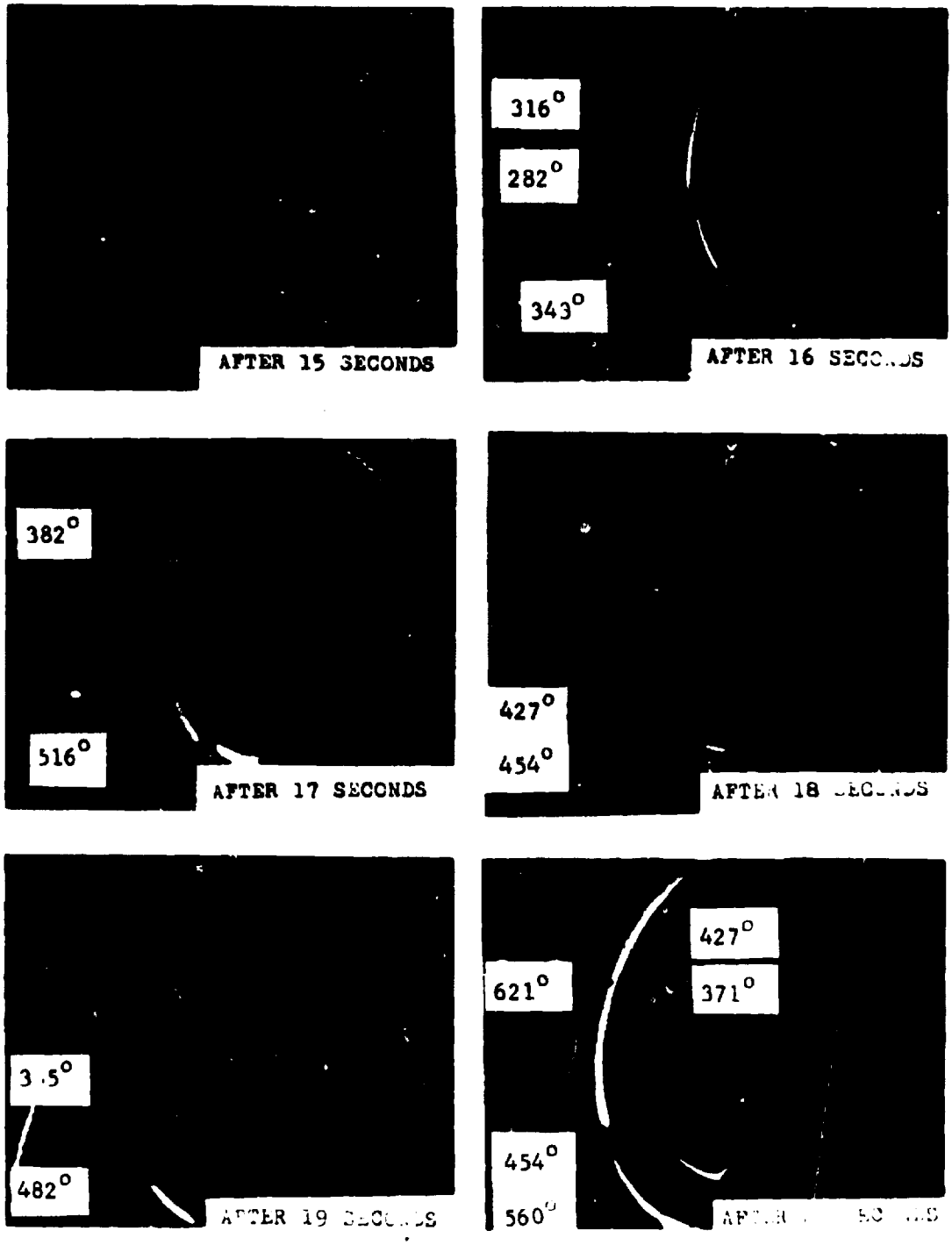

Figure 6. Infrared photographs of brake disk near end of series A braking cycle. Temperatures in °C.

variation in disk surface temperature can be observed between different areas on the contacting surfaces of the disk. The portion of pad-disk interface in actual contact, as indicated by higher temperatures, seems to be continuously shifting, with 25% or less of the nominal pad area in actual contact at any instant.

Further evidence of nonuniform contact between brake pads and disk was found by visual observation of the pads after each 10 runs. Variations in discoloration of the copper-based friction material were noted; sections where contact had been more pronounced appeared dark blue in color, while a grayish-blue was predominant in less-contacting areas. The surface where contact had been most severe appeared to be polished, with the surface oxide showing striations in the circumferential direction.

Similar conclusions of nonuniform contact were reported recently by Peterson and Ho (Ref.2) as a result of their material investigations of used brake pads from an aircraft brake.

In an attempt to analyze the temperatures within the shifting contact areas during braking, a thermomechanical computer simulation was performed in which the thermoelastic deformation and wear of the contacting materials were modelled using the finite element method. The results of that simulation, reported elsewhere (Ref.7), show that the temperature variations of Figures 5a and 5b can be predicted quite well when thermoelastic deformation and wear are integrated into a thermal analysis.

Based on the experimental evidence obtained in this investigation and on the results of the computer simulation, the transient changes in contact area during braking can be explained as follows:

Nonuniform heat generation, due in part to a velocity gradient, causes higher temperatures to occur in some areas of the pad-disk interface. Greater thermal deformation in those areas causes a concentration of contact there, resulting in hot spots or bands. The concentrated contacts get hotter and contact becomes more severe until wear of the contacting area is sufficient to cause contact to shift elsewhere. Thus, thermoelastic instabilities (Ref.6) occur on the contacting surface. The wear rates, as well as the temperatures

and loads, at the concentrated contacts are very high and could be a major contributor to poor brake performance.

Despite the continuously varying contact conditions encountered in this series of tests, the coefficient of sliding friction remained approximately constant at 0.4. The wear rate, measured in terms of amount of pad weight (or mass) worn per 20 second run, also remained constant during the test series. By averaging the wear over the 20 second duration, a wear rate of .018% of pad mass/sec results.

5.2 Results for Modified Pad Configurations

An analysis of the series A test results indicates that a major cause of high temperatures in the standard pad configuration is nonuniform contact between pad and disk. An increase in the uniformity of contact should reduce the surface temperatures and, correspondingly, the wear rate during braking. In an attempt to accomplish this, two design modifications were proposed which would enable the friction pads to adapt themselves better to nonuniform thermal deformation. These modified designs were then tested in a similar manner to the previously discussed test series.

5.2.1 Series C - Slotted Brake Pad

This design modification shown in Figures 7 and 8 consisted of a slot, .06" (.0015 m) deep and .906" (.023 m) wide cut into the sliding surface of the brake pads and several grooves, .125" (.00635 m) wide and .055" (.0014 m) deep cut into the rear surface of the pad. The slot creates two separate rubbing areas, which can adapt somewhat independently to thermal distortions. A further reason for the vertical slot was the finding of Parker and Marshall (Ref.4) that a reduction in length of railway brake blocks in the sliding direction results in more uniform contact and lower temperatures. The rear grooves, which also serve as guide for thermocouple wires, help, along with the slot, to make the brake pad more compliant.

Six thermocouples, in positions 1,2,3,4,7 and 8 (see Figure 4), were used to monitor pad temperatures in this series of tests. Temperature-time curves obtained for this series, averaged over 25 test runs, are shown in Figures 9a and 9b. It can be seen from the curves that there is much less transient

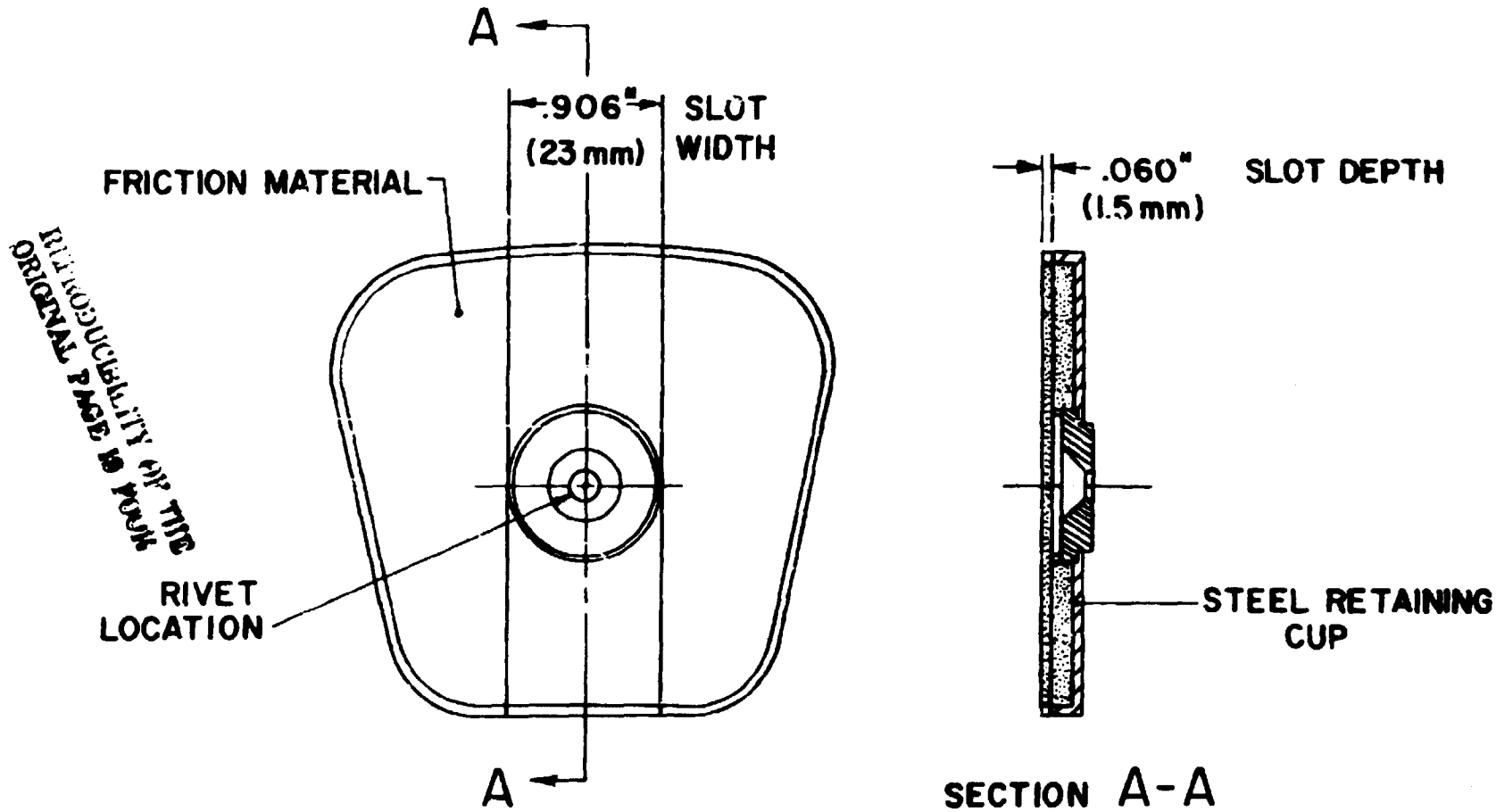

Figure 7 Sketch of slotted front face of brake pad tested in series C

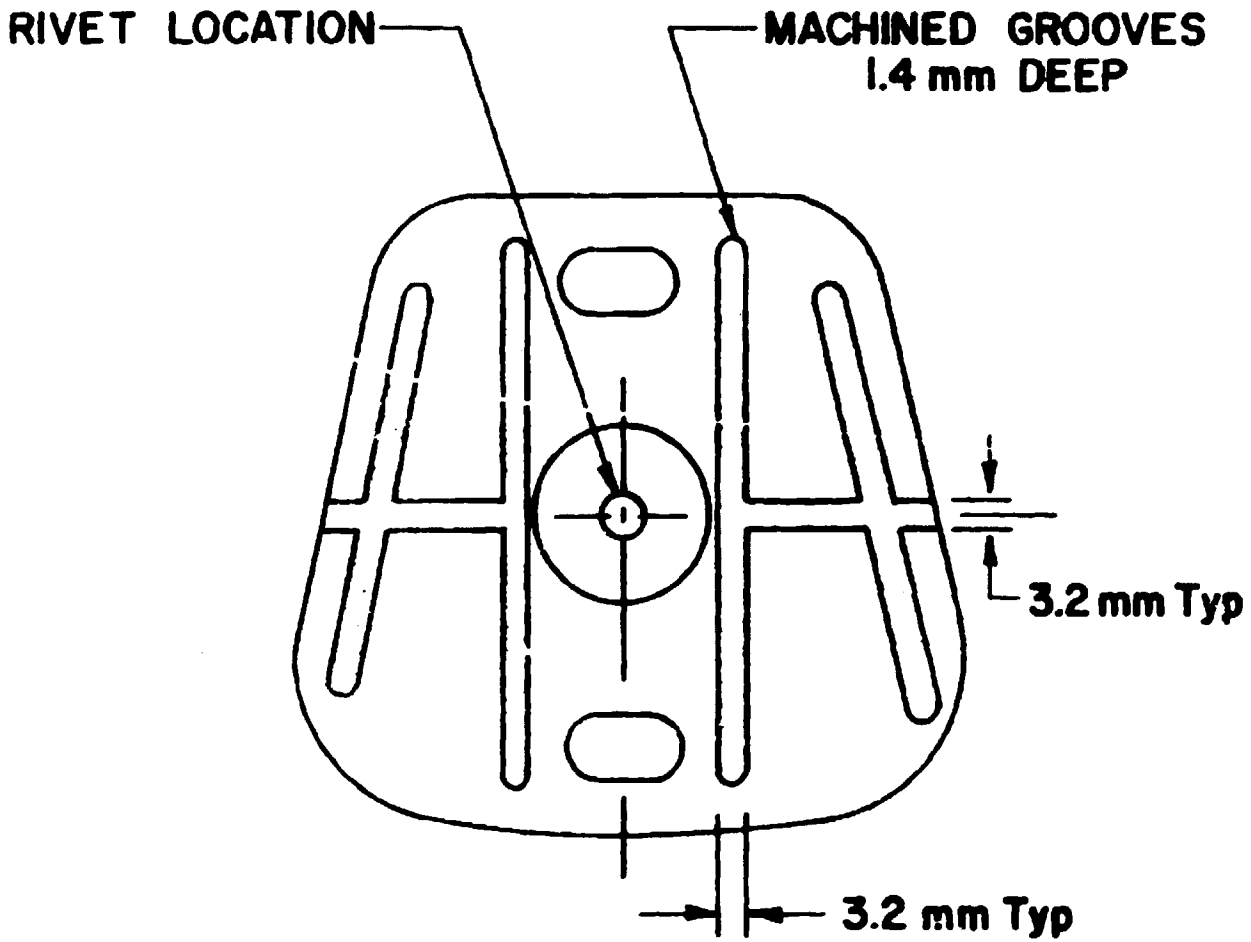

Figure 8 Rear view of slotted brake pad, showing grooves

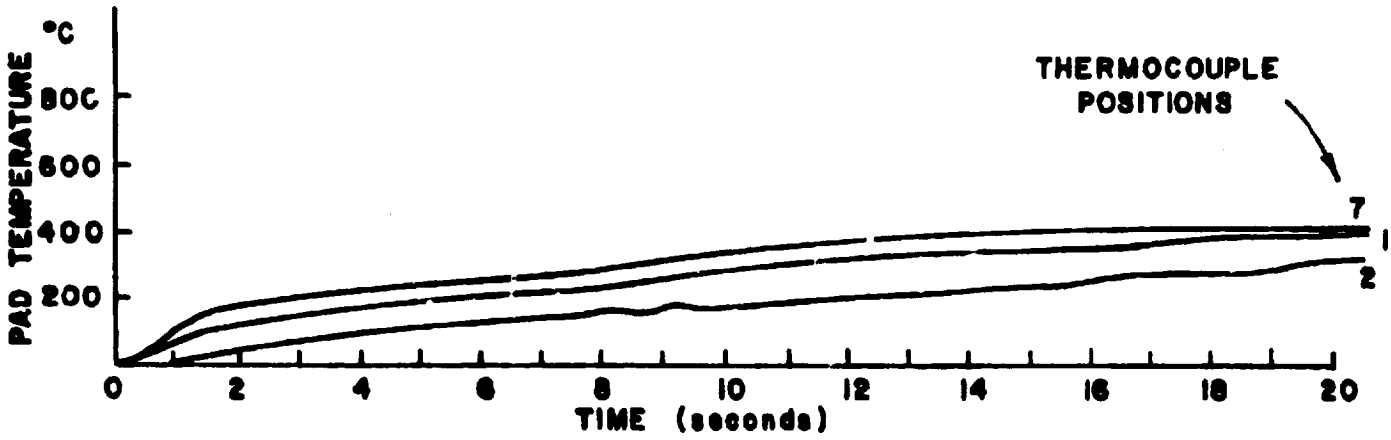

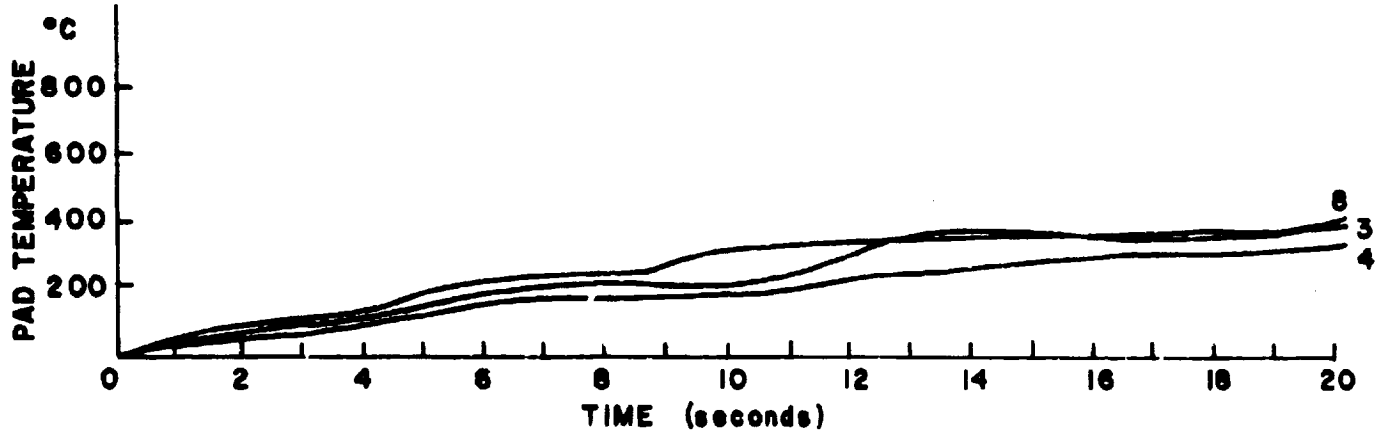

Figures 9a and 9b. Pad near-surface temperature vs. time averaged for 25 test runs. Series C - slotted brake pad.
9a (above) Temperatures for thermocouple positions 1,2,7
9b (below) Temperatures for thermocouple positions 3,4,8

temperature fluctuation than was found for the unmodified pad. Although small radial and circumferential temperature gradients are still noted, the temperature difference between points of different radius (e.g., 1 and 7) is much smaller than for series A.

The temperature-time plots of Figures 9a and 9b indicate clearly that more uniform contact, with fewer contact area changes, was obtained for this modified pad design. Further evidence of this fact results from examination of the magnitude of the temperatures. In spite of the fact that the nominal surface area was decreased by over 31% by slotting the pad, the pad temperatures were up to 30% lower than those for the standard pad. This indicates that the actual contact area was, in fact, greater for this pad design than for the original pad.

As a consequence of the larger actual contact area and lower surface temperatures resulting from grooving and slotting the brake pad, a decrease in wear rate was also noted. The average wear rate was determined to be .010% of pad material/sec, or a 44% reduction in wear rate compared with series A. The average friction coefficient, however, did not change, remaining at about 0.4.

5.2.2 Series R - Ring Spring Brake Pad

For this series it was desired to leave the standard brake pad unchanged, but to attempt to achieve more uniform contact conditions by adding a flexible support behind the pad. A ring spring (Ref.8) was chosen for the support and was designed especially for this application (Ref.9). The ring spring support, shown in Figure 10, was designed to allow the brake pad to adjust freely to non-uniform thermal deformation (see Appendix A).

Two different ring spring assemblies were made and tested. In the first, both spring components were machined from steel. A second ring spring device, made from brass, was then tested to determine the effect of the stiffness of the ring spring material. With both assemblies the mating surfaces of the ring spring components were coated with molybdenum disulfide to reduce friction.

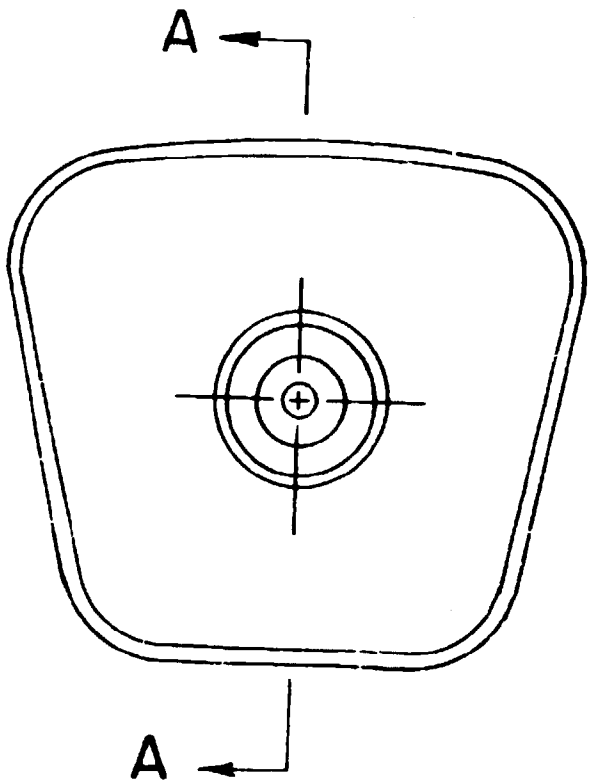

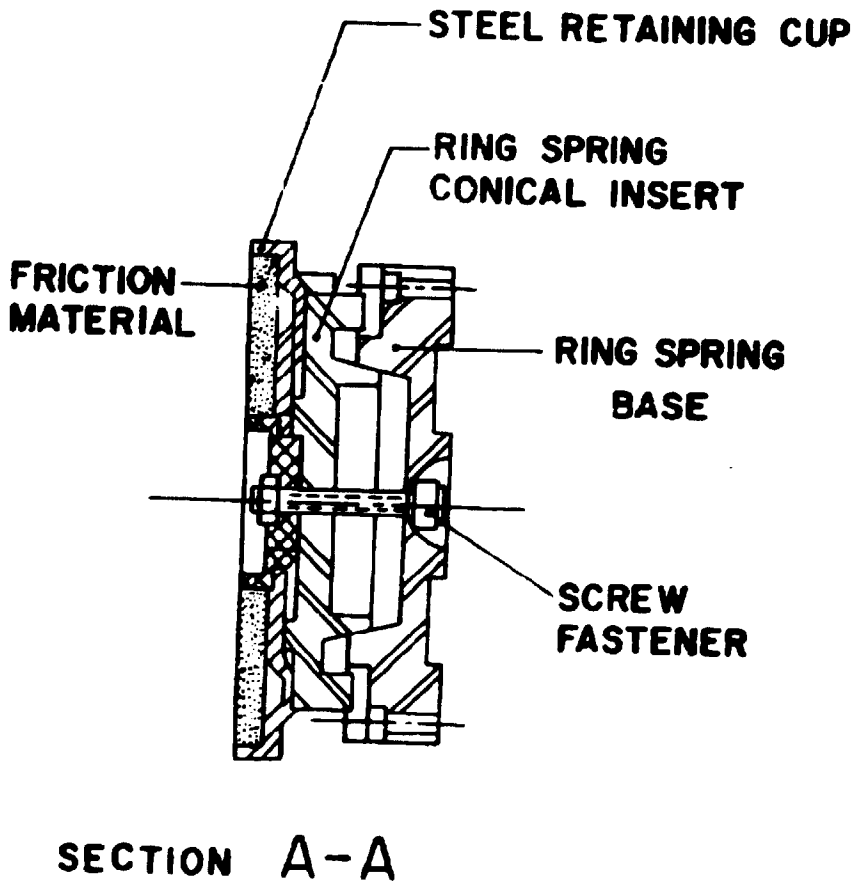

Figure 10 Sketch of ring spring brake pad tested in series R

Thermocouple positions 1,4,5,6,7 and 8 were used in this test series (see Figure 4). The test results showed that for all six positions the temperatures during braking were lower and more uniform than for series A - the standard pad. An indication of this can be seen in Table 2, which shows the average temperatures measured at the end of the 20 second test runs for each configuration. The temperatures obtained with the brass ring spring support were slightly lower than those for the steel spring, indicating that a support material of lower modulus might be more advantageous.

A statistical analysis of the temperature data was performed in order to determine the decrease in temperature at each thermocouple location for the modified pad designs as compared with the standard pad configuration of series A (see Appendix B). These values are presented in Table 3. A 5% significance level (Ref.10) was used in the statistical analysis.

A blank entry in Table 2 indicates either that no temperature measurement was taken at that location or that the computed temperature difference was not significant.

For each of the ring spring devices tested, the value of coefficient of friction was about 0.4, the same as had been found for the earlier test series. A wear rate determination was made only for the steel ring spring tests, and a wear rate of .015% of pad material/sec was calculated. This is a 16% reduction from the rate of series A, but is higher than the value found for series C. The wear rates for all three test series are plotted in Figure 11. In all cases the wear of the steel rotor disk was negligible compared with pad wear.

TABLE 2

COMPARISON OF AVERAGE TEMPERATURES AT END OF 20 SECOND BRAKING CYCLE. TEMPERATURES IN °F (°C)

Thermocouple Location	Series A	Series C	Series R (Steel)	Series R (Brass)
1	1017 (547)	775 (413)	914 (490)	887 (475)
2		754 (401)		
3		600 (316)		
4	1114 (601)	776 (413)	932 (500)	731 (388)
5	949 (509)		880 (471)	874 (468)
6	1019 (548)		812 (433)	797 (425)
7	811 (433)	788 (420)	746 (397)	810 (432)
8	774 (412)	653 (345)	633 (334)	667 (353)

TABLE 3

COMPARISON OF MINIMUM TEMPERATURE DECREASE FROM SERIES A TEMPERATURES AT 5% SIGNIFICANCE LEVEL °F (°C)

Thermocouple Location	Series A	Series C	Series R (Steel)	Series R (Brass)
1		161 (89)	31 (17)	46 (26)
2				
3				
4	Baseline for Comparison	258 (143)	111 (62)	302 (168)
5			13 (7)	9 (5)
6			138 (77)	309 (172)
7				
8		69 (38)	93 (52)	51 (28)

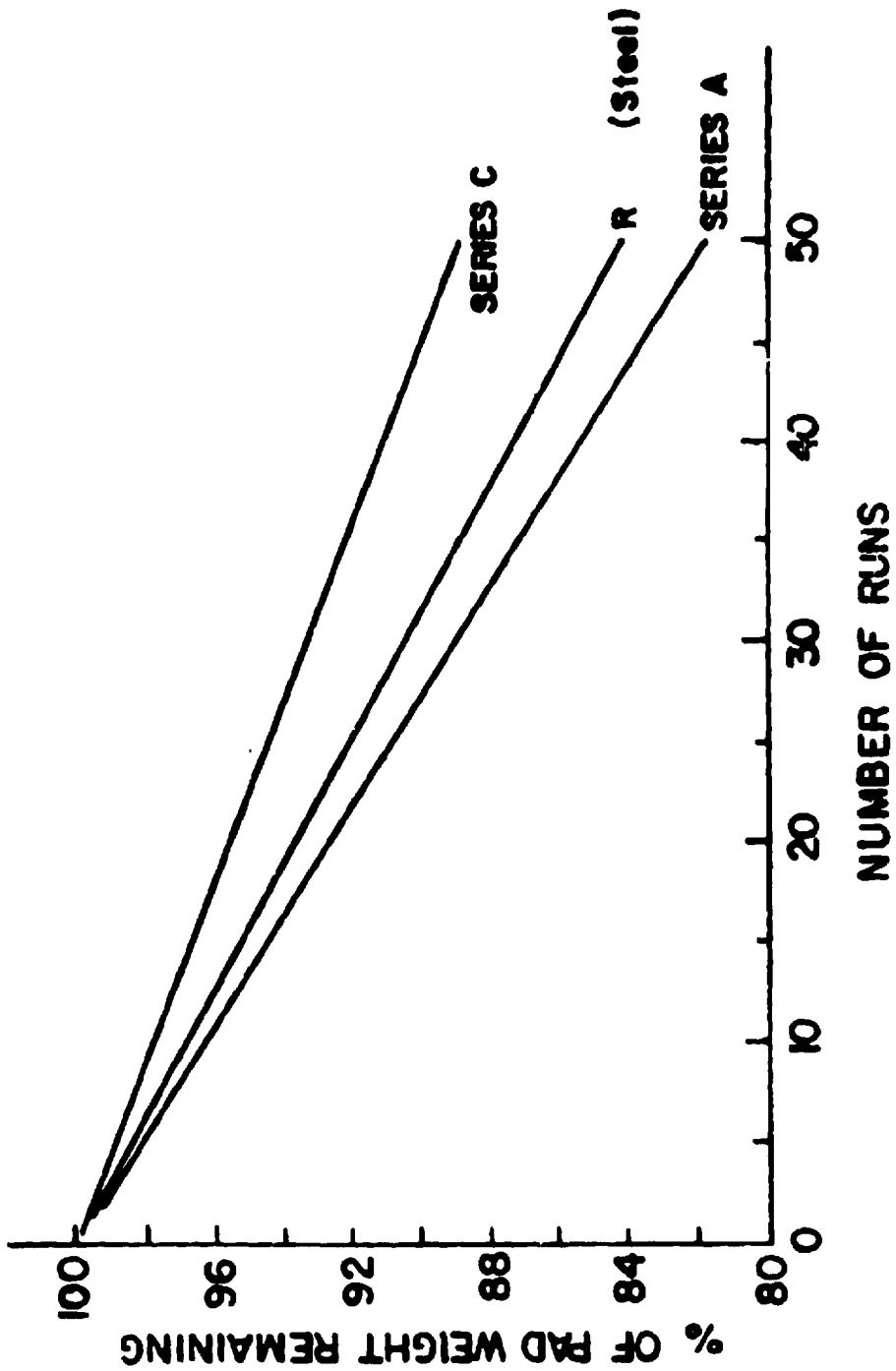

Figure 11 Comparison of wear rates from series A, C, and R

SECTION 6

CONCLUSIONS

1. Continuous monitoring of temperatures in disc brake pads under drag-type testi nditions reveals that a considerable temperature gradient exists between different points on the contacting surface.

2. Temperature measurements and infrared photos both indicate that pad-disk contact is not uniform, with less than 25% of the nominal contact area in actual contact at any instant. Contact areas constantly shift due to nonuniform thermal deformation and wear.

3. Despite the constantly varying contact conditions, the measured coefficient of friction was found to remain approximately constant.

4. Significant decreases in surface temperature and wear rate result from cutting a slot, perpendicular to the sliding direction, on the sliding surface of the friction pad, along with grooves on the rear of the pad. The pad is thus more compliant and better able to adjust to nonuniform deformation, and more uniform contact conditions result. The modification causes no significant change in friction coefficient.

5. Similar improvements in wear rate, surface temperature, and uniformity of contact also result from adding a flexible ring spring support behind the standard friction pad. Better results are obtained when the ring spring support is made from lower modulus materials.

6. Use of either of the proposed design modifications, possibly along with some of the newly developed, high temperature friction materials, could result in safer, longer lasting, and more reliable disk brakes.

APPENDIX A

RING SPRING ANALYSIS

General

Where space is limited and a relatively large amount of energy must be absorbed, a type of spring known as a ring spring may well merit attention by a designer (Ref.8). Applications include shock absorbers for cranes, guns, and vibration dampers for power hammers.

As its name implies, the ring spring consists essentially of a series of rings having conical surfaces and assembled as shown below. When an axial load

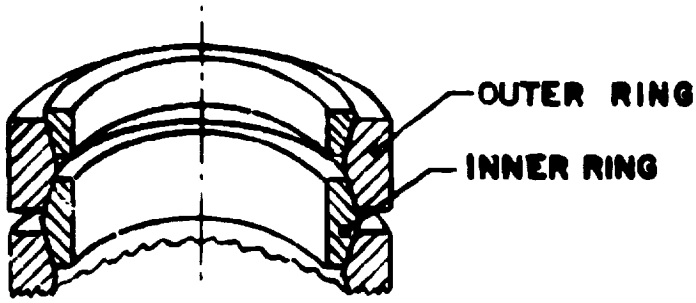

is supplied, sliding occurs along the conical surfaces with the result that the inner rings are compressed and the outer rings extended. In this manner it can be assumed that a uniform distribution of circumferential stress is obtained in the outer and inner rings.

A typical load hysteresis loop for the ring spring is shown below. For purposes of analysis, each conical surface of the ring spring may be considered subject to a total normal force N distributed uniformly around the circumference and a friction force $F = \mu N$, μ being coefficient of friction. Also assumed is that the ring thickness is small compared with the mean diameter. Only half of an inner and outer ring were considered for this application (see Figure 10).

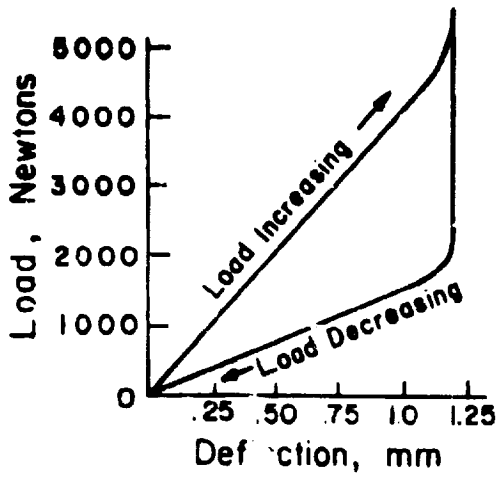

Inner Ring

Consider the inner ring is being compressed so that friction acts in the direction shown below:

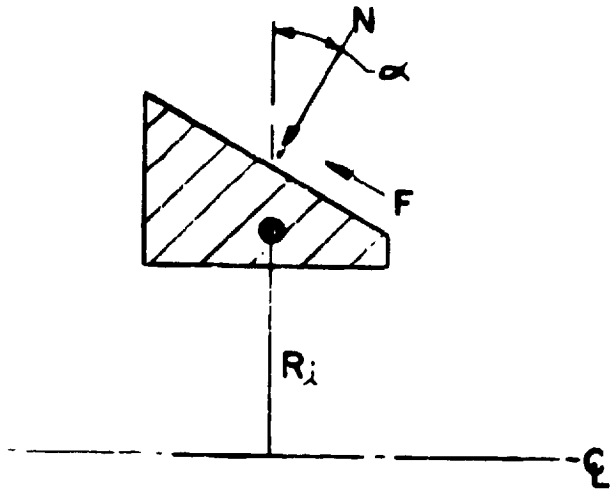

Forces acting on element of ring spring

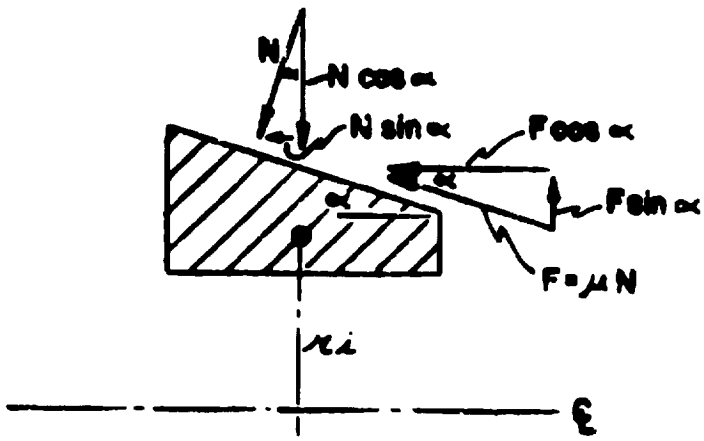

The total radial force acting will be equal to

$$(N \cos \alpha - F \sin \alpha)$$

where α is the angle of taper of the conical surfaces. The radial load p per unit length of the circumferential centerline of the ring will be the total radial force divided by $2\pi r_i$, r_i being the mean radius of the ring, hence

$$p = \frac{(N \cos \alpha - F \sin \alpha)}{2\pi r_i}$$

but $F = \mu N$

$$p = \frac{N(\cos \alpha - \mu \sin \alpha)}{2\pi r_i} \quad . \tag{A1}$$

For a thin ring the compressive stress will be

$$\sigma_c = \frac{p r_i}{A_i} \tag{A2}$$

where A_i is the cross sectional area of the inner ring.

Substituting (A1) into (A2) obtain

$$\sigma_c = \frac{N(\cos \alpha - \mu \sin \alpha)}{2\pi A_i} \tag{A3}$$

The axial load P acting on the spring during the compression stroke is

$$P = N \sin \alpha + F \cos \alpha = N(\sin \alpha + \mu \cos \alpha).$$

Solving for N and substituting in (A3)

$$\sigma_c = \frac{P}{2\pi r_i} \left(\frac{\cos \alpha - \mu \sin \alpha}{\sin \alpha + \mu \cos \alpha} \right) . \tag{A4}$$

Let

$$K = \frac{\tan \alpha(\mu + \tan \alpha)}{1 - \mu \tan \alpha} . \tag{A5}$$

Equation (A4) becomes

$$\sigma_c = \frac{P \tan \alpha}{2\pi A_i K} . \tag{A6}$$

A similar procedure for calculating the circumferential tension stress σ_t in the outer ring is used. This gives

$$\sigma_c = \frac{P \tan \alpha}{2\pi A_o K} \tag{A7}$$

where A_o is the cross-sectional area of the outer ring.

Deflection

To calculate the total deflection of the spring, the radial deflections must be found first. For the inner ring the radial deflection will be approximately equal to $\sigma_c r_m / E$, r_m being the mean radius and E the modulus of elasticity. The axial deflection of the inner ring, δ_i, will be the radial value of $\sigma_c r_m / E$ divided by tan α,

$$\delta_i = \frac{\sigma_c r_m}{E \tan \alpha} \tag{A8}$$

and δ_o, the total axial deflection of the outer ring will be

$$\delta_o = \frac{\sigma_t r_m}{E \tan \alpha} . \tag{A9}$$

Therefore the total axial deflection δ, due to inner and outer ring will be

$$\delta = \delta_o + \delta_i = \frac{r_m}{E \tan \alpha} (\sigma_t + \sigma_c) . \qquad (A10)$$

Using values of σ_c and σ_t given by Eqs.(A6) and (A7) yields

$$\delta = \frac{Pr_m}{2\pi EA_i K} \left(1 + \frac{A_i}{A_o}\right) . \qquad (A11)$$

One further assumption is made on Eq.(A1), that is, the steel insert of the design is the outer ring and that its $A_o >> A_i$, hence $\frac{A_i}{A_o} \to 0$. Therefore,

$$\delta = \frac{Pr_m}{2\pi EA_i K} . \qquad (A12)$$

Design Calculations

1. Ring Spring Brake Backup Pad Using Brass Alloy

Given:

$\sigma_y \approx 3.45 \times 10^8$ N/m^2

$\alpha = .218$ rad, $\tan \alpha = .2217$

$\mu = .09$ (molycoated surfaces)

$K = .069$

$A_i = .9 \times 10^{-5}$ m^2; $E = 9 \times 10^{10}$ N/m^2; $r_m = 1.84$ cm

$P = \frac{2\pi A_i K \sigma_c}{\tan \alpha} = 6070$ Newtons.

Now solve for deflection at this load

$$\delta = \frac{Pr_m}{2\pi EA_i K} = 0.318 \text{ mm.}$$

2. Ring Spring Brake Backup Pad Using C1018 Steel

Given:

$\sigma_y = 3.75 \times 10^8$ N/m^2

$\alpha = .218$ rad; $\tan \alpha = .2217$; $r_m = 1.84$ cm

$\mu = .09$ $\quad A_i = .9 \times 10^{-5}$ m^2

$K = .069$ $\quad E = 20.8 \times 10^{10}$ N/m^2.

Solve for maximum load P, let $\sigma_y \equiv \sigma_c$

$$P = \frac{2\pi A_i K \sigma_c}{\tan \alpha} = 6550 \text{ N.}$$

Then obtain deflection for this load

$$\delta = \frac{P r_m}{2\pi E A_i k} = .15 \text{ mm.}$$

APPENDIX B

STATISTICAL ANALYSIS OF TEMPERATURE DISTRIBUTION

The procedure used for the temperature distribution for the various test series is as follows:

1. The ratio R, of the sample variances for the standard and modified test brake pads was calculated for each thermocouple location. These ratios were then compared against an F statistic. If R fell in the interval,

$$\frac{1}{F_{N_m-1,N_s-1,\alpha/2}} \leq R \leq F_{N_s-1,N_m-1,\alpha/2}$$

where N_s is the sample size of the standard pad data and N_m is the sample size of the modified pad data, then the hypothesis H: $\sigma_s^2 = \sigma_m^2$ would not be rejected. Otherwise, this hypothesis is rejected.

2. If, in step 1, the hypothesis that the variances are equal was not rejected, the t statistic

$$t = \frac{\bar{X}_s - \bar{X}_m - k}{\bar{\sigma}\sqrt{\frac{n_s + n_m}{n_s n_m}}}$$

would be used to test the hypothesis H: $\mu_s > \mu_m + k$, where k is the temperature difference and:

$\mu_s \equiv$ population mean temperature of the standard pad at this particular pad location

$\mu_m \equiv$ population mean temperature of a modified pad at this particular location

$n_s \equiv$ sample size for the standard pad

$n_m \equiv$ sample size for the modified pad

with

$$\bar{\sigma} = \frac{(n_s - 1)S_s^2 + (n_m - 1)S_m^2}{n_s + n_m - 2}$$

where

$S_s^2 \equiv$ sample variance of the standard pad

$S_m^2 \equiv$ sample variance of a modified pad.

If $t > t_{n_s+n_m-2,\alpha}$ then the hypothesis H: $\mu_s > \mu_m + k$ will be rejected. Thus if

$$\frac{\bar{X}_s - \bar{X}_m - k}{\bar{\sigma}\sqrt{\frac{\bar{n}_s + \bar{n}_m}{n_s n_m}}} > t_{n_s+n_m-2,\alpha}$$

then

$$k > -t_{n_s+n_m-2,\alpha}\ \bar{\sigma}\sqrt{\frac{n_s+n_m}{n_s n_m}} + \bar{X}_s - \bar{X}_m \ .$$

3. If, however, in step 1 the hypothesis that the variances are equal, i.e., $\sigma_s^2 = \sigma_m^2$, was rejected then approximate t statistic

$$t' = \frac{\bar{X}_s - \bar{X}_m - k}{\sqrt{\frac{S_s^2}{n_s} + \frac{S_m^2}{n_m}}}$$

is employed with degrees of freedom

$$\nu = \frac{\left(\frac{S_s^2}{n_s} + \frac{S_m^2}{n_m}\right)^2}{\frac{\left(\frac{S_s^2}{n_s}\right)^2}{n_s-1} + \frac{\left(\frac{S_m^2}{n_m}\right)^2}{n_m-1}} - 2 .$$

REFERENCES

1. Hooton, N.A., "Metal-Ceramic Composites in High Energy Friction Applications," Bendix Technical Journal, Vol.2, No.1, pp.55-61, 1969.
2. Peterson, M.B. and Ho, T.L., "Consideration of Materials for Aircraft Brakes," NASA CR-121116, 1972.
3. Jensen, W.A., "Friction Materials,"Machine Design, pp.108-113, 1972.
4. Parker, R.C. and Marshal, P.R., "The Measurement of the Temperature of Sliding Surfaces with Particular Reference to Railway Brake Shoes," Proc. Inst. of Mech. Engrs., Vol.158, pp.209-229, 1948.
5. Sibley, L.B. and Allen, C.M., "Friction and Wear Behavior of Refractory Materials at High Sliding Velocities and Temperatures," ASME Paper No. 61-LUBS-15, 1961.
6. Barber, J.R., "Thermoelastic Instabilities in the Sliding of Conforming Solids," Proc. Roy. Soc., A, Vol.312, pp.381-394, 1969.
7. Kennedy, F.E. Jr., Wu, J.J. and Ling, F.F., "A Thermal, Thermoelastic and Wear Analysis of High-Energy Disk Brakes," NASA-CR-134507, January 1974.
8. Wahl, A.M., "Mechanical Springs," McGraw-Hill Book Co., New York, 2nd Edition, 1963.
9. Santini, J.J., "Effect of Design Factors on the Generation of Surface Temperatures in a Sliding System," D. Eng. Dissertation, Rensselaer Polytechnic Institute, 1973.
10. Burford, R.L., "Statistics: A Computer Approach," Charles E. Merrill Publishing Co., Columbus, Ohio, pp.243-245, 1968.